Measuring seeing and atmospheric time constant by differential scintillations

Andrei Tokovinin

Cerro Tololo Inter-American Observatory, Casilla 603, La Serena, Chile

A simple differential analysis of stellar scintillations measured simultaneously with two apertures opens a possibility to estimate seeing. Moreover, some information on the vertical turbulence distribution can be obtained. A general expression for the *differential scintillation index* for the apertures of arbitrary shape and for finite exposure time is derived, and its applications are studied. Correction for exposure time bias using the ratio of scintillation indices with and without time binning is studied. A bandpass-filtered scintillation in a small aperture (computed as differential-exposure index) provides a reasonably good estimate of the atmospheric time constant for adaptive optics.
OCIS *codes*: 010.1330, 010.1290, 010.1080, 280.7060

1. Introduction

The major characteristic of optical turbulence, seeing, is related to the integral of the turbulence vertical profile[1,2]. Many methods exist for seeing measurements, although only the Differential Image Motion Monitor (DIMM)[3] has proven to be a practical, robust and generally accepted technique. However, a more complete knowledge of turbulence profile is needed to predict the performance of adaptive optical (AO) systems and interferometers. For example, the size of the AO-corrected field of view depends on the turbulence in the upper atmospheric layers, while the required bandwidth of an AO system is related to the atmospheric time constant τ_0 which also can be computed from the profiles of $C_n^2(h)$ and of wind velocity. It is necessary to know the statistics of these atmospheric parameters at a given site in order to design future imaging systems. It is also highly desirable to monitor the relevant atmospheric parameters in real time for more efficient use of AO systems and interferometers.

Current techniques for turbulence profiling include *in situ* sounding with balloon-borne micro-thermometers and remote optical sounding by the SCIDAR method[4]. Both methods are not suitable for continuous monitoring. SCIDAR is based on the spatio-angular statistical analysis of atmospheric scintillation ("flying shadows") produced by double stars and requires a telescope of more than 1 m, while the availability of suitable double stars places severe constraints on the detector sensitivity.

It has been known for a long time that the scintillations of single stars also contain information on the vertical turbulence profile (see a review in[5]). Ochs et al.[6] have built an instrument based on this idea. Although the vertical resolution of single-star profilers is much worse compared to SCIDAR, the availability of bright single stars and the small size of required apertures make this approach attractive for profile monitoring. Atmospheric isoplanatic patch size θ_0 is readily estimated from the scintillation index of single stars observed through a 10-cm aperture[7,8].

Recently we suggested to measure *differential scintillations* of single stars in two concentric apertures[9,10]. This approach permits to obtain low-resolution turbulence profiles and hence to measure seeing and θ_0. In this paper we analyze this technique in more detail and extend it to the temporal analysis which leads to estimates of the atmospheric time constant τ_0. Thus, this approach opens a way to the new generation of simple and robust instruments for complete monitoring of atmospheric turbulence parameters relevant to high angular resolution imaging.

In Sect. 2 the well-known theory of stellar scintillations is extended to the case of differential scintillations. This extension is straightforward, and instead of repeating the derivation we provide only the full complement of formulas needed for the practical implementation of the proposed technique. The influence of aperture shape is investigated in Sect. 3. Application of this technique to turbulence profiling is briefly outlined in Sect. 4, the influence of finite exposure time is investigated in Sect. 5. Finally, in Sect. 6 the new method of τ_0 measurements is described and in Sect. 6 the conclusions are formulated.

2. Normal and differential scintillation indices

The results of the theory of wave propagation in turbulent media[1,2] are used here. The standard theory is based on the weak perturbation (Rytov's) approximation, which is applicable in case of astronomical observations at not very large zenith angles. A point light source at infinity (star) is observed. The distribution of light intensity I in the telescope pupil is related to the relative fluctuations of the wave amplitude χ like $I = I_0 \exp(2\chi)$. Rytov's approximation is valid when $\chi \ll 1$. The *scintillation index* SI, i.e. variance of the natural logarithm of light intensity

$$\sigma_I^2 \approx \left\langle (\ln I - \langle \ln I \rangle)^2 \right\rangle, \tag{1}$$

is calculated as an integral over altitude of the product of refractive index structure constant C_n^2 and some *weighting function* (WF) Q. Angular brackets denote statistical averaging. In the following we use range $z = h \sec\gamma$ instead of altitude h, to take into account observations at some zenith angle γ:

$$\sigma_I^2 = \int_0^{Z_{max}} \mathrm{d}z \; C_n^2(z) Q(z), \tag{2}$$

where the integration is performed from the telescope aperture ($z = 0$) to the maximum distance of turbulence, Z_{max} (Ref. 2, Eq. 8.3). The WF $Q(z)$ is an integral over spatial frequencies of the product of two terms: turbulence spectrum and Fresnel diffraction term. In practice light intensity is always averaged over a finite aperture. It corresponds to additional spatial filtering, as shown by Young[11] (see also Tatarski[1], Roddier[2], p. 343, and Ref. 7), so a third term appears under the integral. These formulae are found in the literature in two forms, depending on whether the spatial frequency f (one over period) or the wavenumber $k = 2\pi f$ are used as the integration variable. First convention is adopted in Refs. 2, 8 and here, while wavenumber convention is adopted in Refs. 7, 9. For the wavelength λ,

$$Q(z) = 9.62\lambda^{-2} \int_0^{\infty} \mathrm{d}f \; f^{-8/3} \sin^2(\pi\lambda z f^2) A(f). \tag{3}$$

In Eq. 3 the integration is performed over the modulus f of the spatial frequency vector (f_x, f_y). While turbulence spectrum and Fresnel term indeed possess angular symmetry, this does not hold for apertures of arbitrary shape. Thus, in the general case the aperture filter must be averaged over the angle before integration over f. Let $W(x, y)$ be the aperture transmission function, and $\tilde{W}(f_x, f_y)$ – its Fourier transform, normalized so that $\tilde{W}(0, 0) = 1$. Transformation to polar coordinates in the spatial frequency plane, $(f_x, f_y) \to (f, \phi)$, and angular averaging lead to the general expression for $A(f)$:

$$A(f) = (2\pi)^{-1} \int_0^{2\pi} \mathrm{d}\phi \; |\tilde{W}(f, \phi)|^2. \tag{4}$$

For example, for a clear circular aperture of diameter d the aperture filter is

$$A_{\mathrm{circ}}(f) = \left[\frac{2 J_1(\pi d f)}{\pi d f} \right]^2, \tag{5}$$

where J_1 is the Bessel function.

Now, suppose that the scintillations are observed simultaneously with two apertures W_1 and W_2, producing light fluxes I_1 and I_2. The *differential scintillation index* (DSI) σ_d^2 can be defined as a variance of the natural logarithm of the ratio of two fluxes:

$$\sigma_d^2 = \left\langle \left(\ln \frac{I_1}{I_2} - \langle \ln \frac{I_1}{I_2} \rangle \right)^2 \right\rangle. \tag{6}$$

The standard theory of small perturbations leading to the Eqs. 2,3 can be easily adapted to this case. It follows from Eq. 6 that $\sigma_d^2 = 4\langle(\chi_1 - \chi_2)^2\rangle$. The Fourier transform of $\chi_1(\vec{x}) - \chi_2(\vec{x})$ is computed as a difference of the Fourier transforms, which, in turn, differ only by aperture filters. Hence the difference $\tilde{W}_1(f_x, f_y) - \tilde{W}_2(f_x, f_y)$ appears instead of $\tilde{W}(f_x, f_y)$. Then, as in the standard theory, the power spectrum is found and the variance is computed by integrating it over frequencies; the square modulus of the aperture filter $|\tilde{W}(f_x, f_y)|^2$ is replaced now by the square modulus of the aperture function's difference. So, for the two apertures W_1 and W_2 the filter function is now

$$A_d(f) = (2\pi)^{-1} \int_0^{2\pi} \mathrm{d}\phi \, |\tilde{W}_1(f, \phi) - \tilde{W}_2(f, \phi)|^2, \tag{7}$$

and Eq. 2 remains valid for the DSI if $A(f)$ is replaced by $A_d(f)$. Differential scintillation can be regarded as a particular form of spatial filtering of the intensity fluctuations in the pupil plane. Ochs et al.[6] also used spatial filtering in their profiler and developed similar formulae.

3. Differential scintillation for various apertures

The weighting functions for differential scintillations (Eqs. 3, 7) were computed for three different configuration of aperture pairs: concentric circular and annular, non-concentric circular, and square (Fig. 1). The results are commented below.

Concentric circular/annular apertures. This configuration (Fig. 1, top) was considered in Ref. 9. Let d be the diameter of the outer annular aperture, and ϵd – diameter of the inner circular aperture. Then the aperture filters are

$$\begin{aligned} \tilde{W}_1(f) &= \frac{1}{1-\epsilon^2}\left[\frac{2J_1(\pi df)}{\pi df} - \epsilon^2 \frac{2J_1(\epsilon\pi df)}{\epsilon\pi df}\right], \\ \tilde{W}_2(f) &= \frac{2J_1(\epsilon\pi df)}{\epsilon\pi df}, \end{aligned} \tag{8}$$

and the filter $A_d(f)$ is

$$A_d(f) = (1-\epsilon^2)^{-2}\left[\frac{2J_1(\pi df)}{\pi df} - \frac{2J_1(\epsilon\pi df)}{\epsilon\pi df}\right]^2. \tag{9}$$

The remarkable property of WFs is that, starting from some altitude, they are practically constant, and thus DSI depends on the integral of C_n^2. The reason for this behavior is illustrated in Fig. 2. In case of normal scintillations, aperture filter admits low spatial frequencies, which dominate in the total integral (3) and increase with layer height. For DSI, $A_d(f)$ has a form of a wide band-pass filter. When it samples the oscillating part of the Fresnel term, the integral becomes independent of the oscillation period, i.e. independent of altitude. This happens when the Fresnel radius $\sqrt{\lambda z}$ is larger than the diameter of the inner aperture ($\sqrt{\lambda z} = 2.2$ cm for $\lambda = 500$ nm and $z = 1$ km).

Non-concentric apertures. It is of practical interest to consider the case of DSI measurements with two symmetric apertures which do not have a common center. Such situation may occur when a telescope with a central obscuration is used, and inner aperture is selected in the unobstructed outer part of the pupil.

Let $\tilde{W}_1(f)$ and $\tilde{W}_2(f)$ be the real Fourier-transforms of the two rotationally symmetric (e.g. circular) apertures. Without loss of generality we suppose that inner aperture is shifted along the x axis by some amount Δ. In the general Eq. 7 the integrand will be equal to $\tilde{W}_1^2 + \tilde{W}_2^2 - 2\tilde{W}_1\tilde{W}_2\cos(2\pi f\Delta\cos\phi)$. Angular averaging leads to the Bessel function:

$$A_d(f) = \tilde{W}_1^2(f) + \tilde{W}_2^2(f) - 2\tilde{W}_1(f)\tilde{W}_2(f)J_0(2\pi\Delta f). \tag{10}$$

It turns out that even a small amount of de-centering changes the shape of $A_d(f)$ at low frequencies. Indeed, for concentric apertures $A_d(f)$ is proportional to f^4 at small f, while de-centering adds a term of the order of f^2. As

a consequence, more turbulence power at low frequencies is transmitted. Qualitatively, low-frequency component of the intensity variations can be represented as a gradient over aperture. For concentric apertures the gradient does not change the ratio of transmitted intensities, whereas for de-centered apertures it does. Calculations show that the DSI WF with de-centering is increasing with altitude, contrary to the case of concentric apertures.

In Fig. 1 (middle) we illustrate the effect of a small (0.1 of outer diameter) de-centering on the WF. The calculations were done for a pair of circular apertures (i.e. the central obscuration of the outer aperture was neglected). For a de-centering of 0.25, as would be appropriate if the outer zone of a cassegrain telescope pupil were used, the WFs completely change their character.

Square apertures. If the scintillation pattern is observed by a detector with square pixels, it is natural to consider square apertures. Applying Eq. (7) to a case of square aperture of the size ϵd inside a square of the size d ("concentric" square apertures), we obtain

$$\tilde{W}_1(f,\phi) = (1-\epsilon^2)^{-1}\left[\mathrm{sinc}(df\cos\phi)\mathrm{sinc}(df\sin\phi) - \epsilon^2\mathrm{sinc}(\epsilon df\cos\phi)\mathrm{sinc}(\epsilon df\sin\phi)\right],$$
$$\tilde{W}_2(f,\phi) = \mathrm{sinc}(\epsilon df\cos\phi)\mathrm{sinc}(\epsilon df\sin\phi), \qquad (11)$$

where $\mathrm{sinc}(x) = \sin(\pi x)/(\pi x)$. Hence,

$$A_d(f) = (1-\epsilon^2)^{-2}(2\pi)^{-1}\int_0^{2\pi} \mathrm{d}\phi\,[\mathrm{sinc}(df\cos\phi)\mathrm{sinc}(df\sin\phi) - \mathrm{sinc}(\epsilon df\cos\phi)\mathrm{sinc}(\epsilon df\sin\phi)]^2. \qquad (12)$$

The numerical computation of $A_d(df)$ shows that at small arguments it grows like f^4, similar to the case of annular apertures. At large f it falls asymptotically as f^{-3}, showing quasi-periodic oscillations typical of sinc function. We approximated this function by a polynomial for $df < 36$ and set it to zero for larger arguments. Corresponding WFs are shown in Fig. 1 (bottom). They are qualitatively very similar to the DSI WFs for circular/annular apertures.

4. Estimation of seeing and turbulence profile from DSI

It is known[1,2] that seeing it directly related to the integral of $C_n^2(z)$ over z. This integral over all altitudes except the lowest ones can be directly derived from DSI, because the WFs are constant. Thus, a seeing in the free atmosphere (i.e. excluding boundary and ground layers) can be measured, which is of certain interest in site characterization. First actual DSI measurements of free-atmosphere seeing are reported in Ref. 10.

The full integral (and full seeing) can also be measured if a principle of Generalized SCIDAR is used[4]. The double aperture can be optically conjugated to some negative altitude H, adding a virtual turbulence-free propagation path (Fig. 3). Thus, a ground layer also produces some scintillation in this regime. The WFs are shifted to the left, and if H is chosen large enough, a constant WF over the whole range is obtained. However, a too large H would increase scintillation beyond the applicability of the weak perturbation theory; here we use shifts of less than 1 km, far from saturating scintillations in real situations.

The theory of Generalized SCIDAR is valid only for an ideal telescope with infinite aperture. Practically, the telescope must be larger than the outer aperture diameter d by at least 2 Fresnel radii, $2\sqrt{\lambda|H|}$. Optical quality must be diffraction-limited at a spatial scale d, or image quality better than λ/d. An imperfect tracking would move the projection of the aperture on telescope pupil, requiring an extra telescope size margin of $2\alpha H$ for tracking errors of $\pm\alpha$. It means that small values of H are preferable. Fortunately, $H = -1$ km is sufficient for seeing measurement with a pair of 2 and 4 cm apertures, requiring a telescope of 10-15 cm size with image quality better than $2''$ and tracking errors within few arcseconds.

The "cut-off" altitude of the DSI WF depends on d. With aperture pairs of different diameters it is hence possible to get information on turbulence intensity in different slabs of atmosphere, — a turbulence profile. Unfortunately, the cut-off is rather shallow, leading to poor vertical resolution. Generalized regime must also be used to estimate turbulence in the lowest layers. Our preliminary studies indicate that with a set of SIs and DSIs measured with 4 concentric circular/annular apertures of suitable size conjugated sequentially to the pupil plane and to -1 km, it is possible to obtain a vertical resolution $\Delta z/z \sim 0.5$.

The issue of signal-to-noise ratio achievable with stellar sources was addressed in Ref. 5. It is most critical for the smallest apertures, where the WFs are smaller (less scintillation signal) and the photon flux is also less. For example, the pair of 2 cm and 4 cm apertures has $Q \approx 3\cdot 10^{10}$ m$^{-1/3}$ (Fig. 1, top). A good seeing (0.5 arcsec) corresponds

to the C_n^2 integral of $2.2 \cdot 10^{-13}$ m$^{1/3}$, leading to a DSI of 0.0066. Let us suppose that this signal is measured with elementary exposure time of 1 ms (see below) and that the fluctuations are averaged during 1 min. (a total of $M = 60000$ samples). If the stellar source of magnitude 2.5 is used (there is always such star not far from zenith), each 1 ms exposure would give about $N = 300$ detected photons in the 2 cm aperture (a total quantum efficiency of 10% and a spectral bandwidth of 100 nm were assumed). Relative variance of flux due to photon noise would be $1/N \approx 0.003$, two times less than the scintillation signal. Statistical averaging of M independent samples leads to the relative error of $M^{-1/2} \approx 0.4\%$ in the estimated variance, which means that the error caused by photon noise would amount to only 0.2% of the scintillation signal. The major source of uncertainty in the DSI measurements is not the photon noise but the statistical noise of the scintillation itself, for which 1 ms samples are not totally independent and the relative error is larger than $M^{-1/2}$. This was confirmed experimentally[10]. Still, measuring DSI with 1% relative accuracy in 1 min. is realistic. Further discussion of single-star turbulence profilers is outside the scope of this work.

5. Finite exposure time

The calculations above assumed that scintillations are registered with infinitely small time. In reality, the exposure time is finite, and this introduces a non-negligible bias in the SI or DSI measurements. This bias is calculated below.

Integrating stellar light during a finite exposure time τ is equivalent to a spatial smoothing of the scintillation pattern over a distance $V\tau$, if a single turbulent layer moving with a velocity V is considered. Here the Taylor approximation of frozen turbulence is used, which is good for small (< 0.1 s) exposure times when internal motions in a layer can be neglected. Without loss of generality, we assume that vector V is parallel to the x axis (for circular apertures all other factors are symmetric).

Smoothing in x-direction is described by a convolution with a rectangle of the width $V\tau$, hence the scintillation power spectrum is multiplied by the additional factor $|\tilde{W}_\tau(f_x, f_y)|^2$, where

$$\tilde{W}_\tau(f_x, f_y) = \mathrm{sinc}(f_x V\tau). \tag{13}$$

Replacing f_x by $f\cos\phi$ and using (4), the additional spatial filter $A_\tau(f)$ caused by time averaging is obtained:

$$A_\tau(f) = (2\pi)^{-1} \int_0^{2\pi} \mathrm{d}\phi\, \mathrm{sinc}^2(fV\tau\cos\phi) = \mathcal{T}_1(V\tau f), \tag{14}$$

where the function $\mathcal{T}_1$ was introduced:

$$\mathcal{T}_1(\zeta) = (2\pi)^{-1} \int_0^{2\pi} \mathrm{d}\phi\, \mathrm{sinc}^2(\zeta\cos\phi). \tag{15}$$

We could not find an analytic solution of this definite integral in the tables[12] and computed it numerically. The function $\mathcal{T}_1(\zeta)$ deviates from 1 quadratically for $\zeta \ll 1$, then falls rather rapidly, $\mathcal{T}_1(1) = 0.309$, and tends to $(\pi\zeta)^{-1}$ for $\zeta \gg 1$. The change of variables $y = (1+\zeta^2)^{-0.5}$ maps the $(0,\ \infty)$ interval in ζ into $(0,\ 1)$ interval in y. The function $\mathcal{T}_1(y)$ can be approximated by the 8-th degree polynomial on this interval with an absolute error of ± 0.005 or a relative error of $\pm 3\%$; moreover, such approximation has correct asymptotic behavior at large and small ζ. The coefficients of $\mathcal{T}_1$ as power series in y from y^0 to y^7 are 0, 0.2245, 2.0247, -15.7485, 58.8973, -109.331, 97.6583, -32.7291.

The above derivation is valid for apertures with a circular symmetry and is applicable both to normal SI and to DSI. The SI reduction produced by a single layer at a range z due to finite exposure time, $R(\tau, z)$, is thus equal to

$$R(\tau, z) = \sigma_I^2(\tau, z)/\sigma_I^2(0, z) = Q_\tau(z)/Q(z) \tag{16}$$

for any symmetric aperture filter A. Here Q is the WF given by Eq. 3, and Q_τ – the WF computed from the same equation by replacing A with AA_τ. This bias slightly depends on the range z for the SI, and is z-independent for DSI at those altitudes where WF is constant.

In Fig. 4 the exposure time bias is calculated for a single layer, both for normal and differential indices. It depends only on the total shift $V\tau$. At small shifts the bias deviates from 1 quadratically, while for large shifts it is proportional to $(V\tau)^{-1}$. It has been suggested to correct the exposure bias by computing the SI with reduced time resolution (from binned data). A ratio $r = \sigma^2(2\tau)/\sigma^2(\tau)$ contains some information on the scintillations time constant. However, at $V\tau \gg d$ the ratio of indices r tends to a constant value of 0.5, and hence becomes useless for bias correction; only at $r > 0.6$ it is feasible to expect a reasonable correction.

A simple linear extrapolation (correction 1) was proposed in Refs. 10, 8:

$$\sigma^2(\tau = 0) \approx 2\sigma^2(\tau) - \sigma^2(2\tau) = \sigma^2(\tau)(2 - r). \tag{17}$$

The corresponding corrected bias is plotted in Fig. 4 in dotted lines. It is evident that it over-corrects at small $V\tau$ by $\sim 10\%$ and under-corrects at larger $V\tau$. A somewhat better correction (correction 2, dashed lines in Fig. 4) is given by

$$\sigma^2(\tau = 0) \approx \sigma^2(\tau)/(1.4 - 0.4/r). \tag{18}$$

Using five profiles measured at Cerro Pachon in October 1998 (Ref. 13), we computed the contributions of individual layers to the total DSI, and integrated them to obtain the DSIs with different exposure times (Eq. 6 with the weighting function Q_τ instead of Q). One such example is shown in Fig. 5. It is immediately apparent that the bias varies significantly with altitude, following $V(h)$. Strong turbulent layers are often associated with a velocity shear, and the resulting exposure time bias is less than one would expect for a single layer moving with the maximum velocity. The calculated bias for a DSI with 4 and 2 cm aperture pair is given in Table 1 for the 5 profiles. The two proposed corrections are applied, and the bias remaining after correction is given in the last two columns of Table 1. As expected, both corrections are accurate within 5%, the first one is slightly over-correcting, and the second one is under-correcting.

Our conclusion is that the ratio r of the two indices computed with raw and binned data is a good diagnostic of the exposure time bias and, to a certain extent, is useful for recovering from it with an accuracy of few per cent. However, such de-biasing also increases the noise in the indices by as much as 2 times.

6. Differential exposure scintillation and time constant

The adaptive optics time constant τ_a is related to the C_n^2-weighted integral of the wind velocity modulus $V^{5/3}$ over range[14]:

$$\tau_a = 0.314 r_0/\bar{V} = 0.057\lambda^{6/5} \left[\int_0^{Z_{max}} \mathrm{d}z \; C_n^2(z) V^{5/3}(z) \right]^{-3/5}. \tag{19}$$

Is it possible to measure τ_a using scintillations? At first sight, the task seems formidable: not only must we have a WF which does not depend on altitude, but this function must increase as $V^{5/3}$. The effect of exposure time is just opposite, decreasing weight for faster wind. However, a new idea can be tried.

The principle of differential scintillations can be applied not only to different apertures, but also to different exposure times, by computing the *differential exposure scintillation index* (DESI) σ_{de}^2 (variance of the logarithm of intensity ratio with different exposure times):

$$\sigma_{de}^2 = \left\langle \left(\ln \frac{I(\tau_1)}{I(\tau_2)} - \langle \ln \frac{I(\tau_1)}{I(\tau_2)} \rangle \right)^2 \right\rangle. \tag{20}$$

The σ_{de}^2 can be viewed as a variance of the bandpass-filtered scintillation signal with suppressed low frequencies. It is convenient to bin the adjacent 3 values of $I(t)$ data, which gives the exposure ratio $\tau_1/\tau_2 = 3$. Corresponding aperture filter is obtained from the general Eq. 7 by putting there two sinc functions. The result is $A_{de}(f) = \mathcal{T}_2(V\tau f)$, where

$$\mathcal{T}_2(\zeta) = (2\pi)^{-1} \int_0^{2\pi} \mathrm{d}\phi \; [\mathrm{sinc}(3\zeta\cos\phi) - \mathrm{sinc}(\zeta\cos\phi)]^2. \tag{21}$$

The numerical technique is similar to that used for $\mathcal{T}_1$: ζ is replaced by a new variable $y = [1+(3\zeta)^4]^{-1/4}$ and $\mathcal{T}_2(y)$ is approximated by an 8-th degree polynomial with the coefficients 0.0189, -0.3308, 15.885, -108.45, 344.32, -532.12, 390.27, -109.59. This approximation is good to ± 0.015. Alternatively, a relation $\mathcal{T}_2(\zeta) = \frac{5}{3}\mathcal{T}_1(\zeta) - \frac{8}{3}\mathcal{T}_1(2\zeta) + \mathcal{T}_1(3\zeta)$ can be employed, as pointed out by the Referee. For control, $\mathcal{T}_2(1) = 0.201$.

Similarly to DSI, the WFs have two regimes. When the shift $V\tau$ is less than the Fresnel radius $\sqrt{\lambda z}$, the DESI WF is independent of altitude because the oscillating part of the Fresnel term is averaged and low frequencies are cut off. In this regime the WFs increase with V, roughly proportionally to $V^{5/3}$ (Fig. 6). The second regime is for large shifts, $V\tau > \sqrt{\lambda z}$, when WFs diminish again, because $A_{de}(f)$ samples the Fresnel factor near coordinate origin where it is small.

Additional aperture averaging complicates the things unless $d \ll \sqrt{\lambda z}$, which is difficult to achieve. Aperture influence becomes significant for $V\tau \le d$, and leads to a decrease of WF faster than $V^{5/3}$ at small V.

In Fig. 7 the DESI WFs are given for a 1 cm diameter circular aperture and exposure times of 1 and 3 ms. Proportionality to $V^{5/3}$ implies that for a 2-fold increase in V the weights should increase by 3.17 times. This is achieved for altitudes above 10 km and wind speeds between 20 and 40 m/s.

Let us suppose that a small aperture is conjugated to some negative altitude. Wind speed at the ground is not likely to exceed 20 m/s (at higher wind telescopes are not operational anyway), and ground layer contribution to the integral (19) will be estimated correctly. Higher layers may move faster, but pose less problems owing to the increased Fresnel radius. So, there is a hope that atmospheric time constant τ_{de} can be estimated using the relation

$$\tau_{de} = K \; [\sigma^2_{de}]^{-3/5}. \tag{22}$$

By choosing the appropriate proportionality constant K, we might obtain $\tau_{de} \approx \tau_a$ in a certain range of parameters. How good is this approximation?

We took 5 real profiles of $C_n^2(h)$ and $V(h)$ measured by balloons at Cerro Pachon[13] and computed τ_a from Eq. 19. The DESIs were computed from the same profiles for a 2-cm circular aperture conjugated to -1 km. Corresponding τ_{de} are compared to τ_a in Fig. 8 with an empirically adjusted constant $K = 0.175$ (asterisks). The agreement is even better than expected! Of course, it can be worse for some less "cooperative" profiles. To increase further the range of time constants, the same profiles were processed with velocities increased or decreased by two times. For high velocities (small τ_a, pluses) the agreement is still good, but large τ_a (slow wind) seem to be systematically over-estimated: σ^2_{de} is too small because of finite aperture size. However, for large τ_a the data can be binned to double the exposure time, thus recovering the accuracy of this method.

7. Conclusions

A new concept of differential scintillation index for two different apertures (DSI) and for two different exposure times (DESI) is introduced. A generalization of the standard weak-perturbation theoretical results to this case is straightforward and implies only a change of the aperture filtering function: instead of a low-pass spatial filter, it becomes a bandpass filter. The new property of DSI for concentric apertures is its independence of altitude over a certain range. It permits to use DSI for the measurement of seeing and for the crude study of turbulence vertical profile. Similarly, DESI offers a practical way to measure atmospheric time constant with a reasonable accuracy of 10% or better.

This approach to turbulence measurements requires an aperture of moderate size (less than 15 cm) and few light detectors. Telescope vibrations are not critical. A new generation of robust site-testing equipment and seeing monitors based on this principle may be designed. As a caveat, it should be noted that scintillations sample phase perturbations of centimetric size, and an extrapolation of results to large spatial scales inevitably relies on turbulence models. This is a common feature of all current techniques for turbulence characterization like SCIDAR, DIMM or balloons. Thus, although a rather complete set of atmospheric optical parameters (seeing, profile, isoplanatic

angle, time constant) can be derived from scintillations, additional techniques (like GSM[8]) are needed to study the low-frequency turbulence which is important for large-aperture telescopes and interferometers.

ACKNOWLEDGMENTS

The author thanks J. Vernin and A. Ziad from the Nice University for providing the digitized profiles and for useful discussions. He is grateful to M. Sarazin and N. Hubin: without their stimulating input this work would have never been done. The contribution of two Referees in improving the clarity of presentation is acknowledged.

---

1. V.I. Tatarsky, "Wave propagation in a turbulent medium", (Dover Publ., Inc., New York, 1961).
2. F. Roddier, " The effects of atmospheric turbulence in optical astronomy", in *Progress in Optics,* E. Wolf, ed. (North-Holland, Amsterdam, 1981), Vol. XIX, pp. 281-376.
3. M. Sarazin and F. Roddier, "The ESO differential image motion monitor", Astronomy and Astrophys., **227,** 294-300 (1990)
4. A. Fuchs, M. Tallon, and J. Vernin, "Focusing on a Turbulent Layer: Principle of the Generalized SCIDAR", Publ. Astron. Soc. Pacif., **110,** 86-91 (1998).
5. A.A. Tokovinin, "Study of single-star turbulence profilers", ESO Report VLT-TRE-UNI-17416-0008 (European Southern Obs., Garching, 1998).
6. G.R. Ochs, Ting-i Wang, R.S. Lawrence, and S.F. Clifford, "Refractive-turbulence profiles measured by one-dimensional spatial filtering of scintillations", Appl. Opt., **15,** 2504-2510 (1976)
7. J. Krause-Polstorf, E.A. Murphy, and D.L. Walters, "Instrumental comparison: corrected stellar scintillometer versus isoplanometer", Appl. Opt., **32,** 4051-4057 (1993).
8. A. Ziad, R. Conan, A. Tokovinin, F. Martin, J. Borgnino, "From the Grating Scale Monitor (GSM) to the Generalized Seeing Monitor (GSM)", Appl. Opt., **39,** 5415-5425 (2000).
9. A.A. Tokovinin, "A new method to measure the atmospheric seeing", Pis'ma v Astron. Zhourn., **24,** 768-771 (Astron. Letters, **24,** 662-664) (1998).
10. V.G. Kornilov and A.A. Tokovinin, "Measurement of the turbulence in the free atmosphere above Maidanak", Astronomy Reports, **45,** 395-408 (2001).
11. A. T. Young, "Aperture filtering and saturation of scintillations", JOSA, **60,** 248 (1970).
12. Referee has pointed out that $\mathcal{T}_1(\zeta) = {}_1F_2(\frac{1}{2};\frac{3}{2};2;-\pi^2\zeta^2)$, where ${}_1F_2$ is the generalized hypergeometrical function, cf. I.S. Gradshteyn and I.M. Ryzhik, "Tables of Integrals, Series and Products", Academic Press Inc., London, Eq. 9.14.1, p. 1045 (1980). We verified that our numerical computation agrees with the series expression for ${}_1F_2$ in the domain where the series converge.
13. J. Vernin, A. Agabi, R. Avila, M. Azouit, R. Conan, F. Martin, E. Masciadri, L. Sanchez, and A. Ziad, "1998 Gemini site testing campaign. Cerro Pachon and Cerro Tololo", Gemini Report RPT-AO-G0094, http://www.gemini.edu/ (2000).
14. F. Roddier, ed., "Adaptive optics in astronomy" (Cambridge Univ. Press, Cambridge, 1999), p. 15.

Table 1. DSI exposure time bias for 5 profiles at Cerro Pachon

Profile	$R(1ms)$	$R(2ms)$	r	Correction 1	Correction 2
155	0.832	0.628	0.755	1.035	0.956
156	0.834	0.615	0.737	1.053	0.972
158	0.895	0.744	0.831	1.046	0.974
160	0.771	0.590	0.765	0.953	0.879
162	0.795	0.560	0.704	1.030	0.955

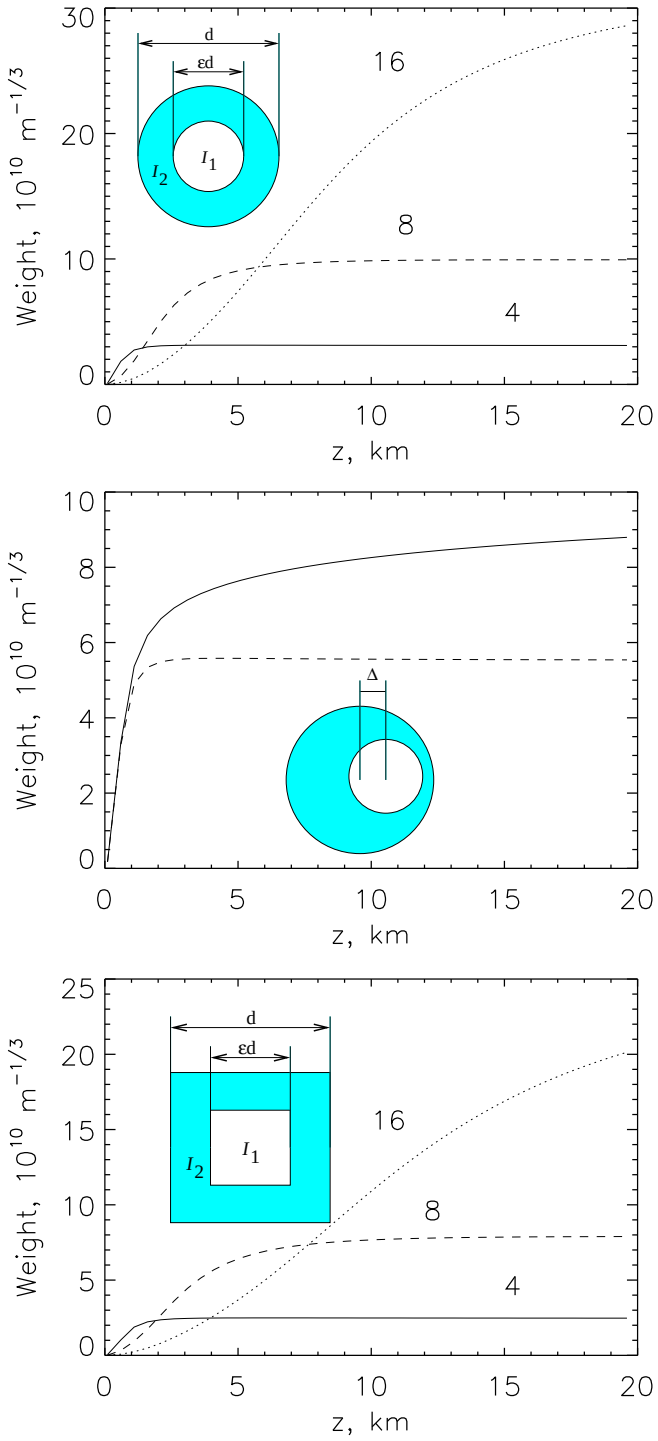

Fig. 1. The DSI weighting functions are plotted for three different configurations of the two apertures. Calculations are made for $\lambda = 500$ nm, $\epsilon = 0.5$, and aperture size d of 16 cm, 8 cm, and 4 cm. Top – circular concentric apertures. Middle – WFs for two clear circular apertures with $d = 4$ cm, $\epsilon = 0.5$ which are concentric (dashed line) or de-centered by $\Delta = 0.1d$. Bottom – square concentric apertures.

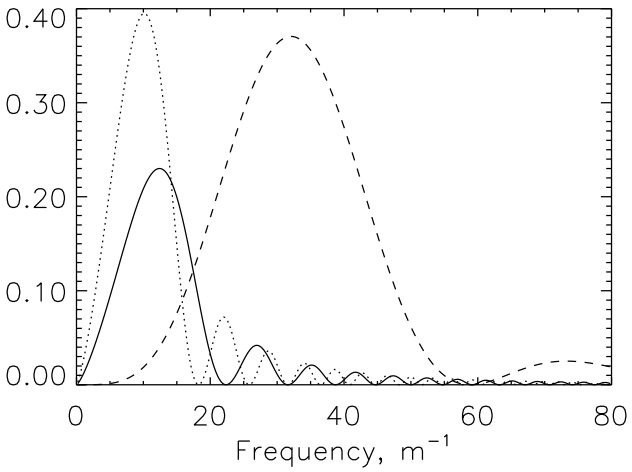

Fig. 2. Weighting function for DSI is given by the integral of three-terms product over spatial frequency (Eq. 3). The product of turbulence spectrum $f^{-8/3}$ and Fresnel factor $\sin^2(\pi\lambda z f^2)$ is plotted for layer altitudes of 4 km (full line) and 6 km (dotted line). The aperture filter for differential scintillations with 4 cm and 2 cm apertures (dashed line) cuts off low frequencies and averages the oscillations, leading to an altitude-independent WF.

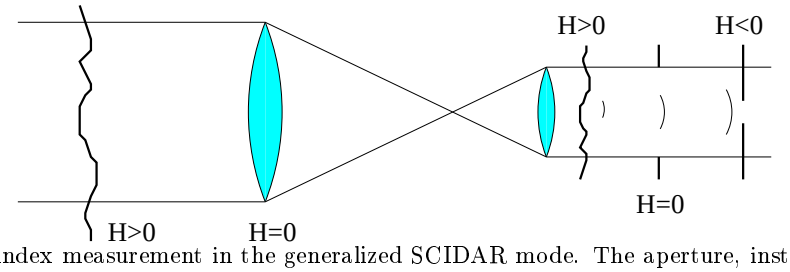

Fig. 3. Scintillation index measurement in the generalized SCIDAR mode. The aperture, instead of being placed in the exit pupil ($H = 0$), is optically conjugated to some other altitude H. A turbulent layer gives no scintillation if aperture is conjugated to it, but gives increased scintillation if $H < 0$, as though an extra propagation path was added. The aperture must be smaller than exit pupil in order to avoid diffraction at the pupil edge.

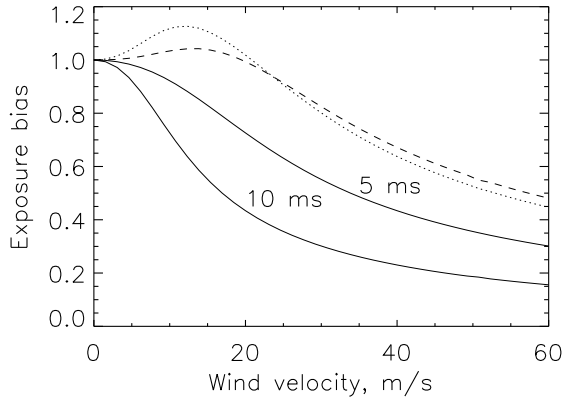

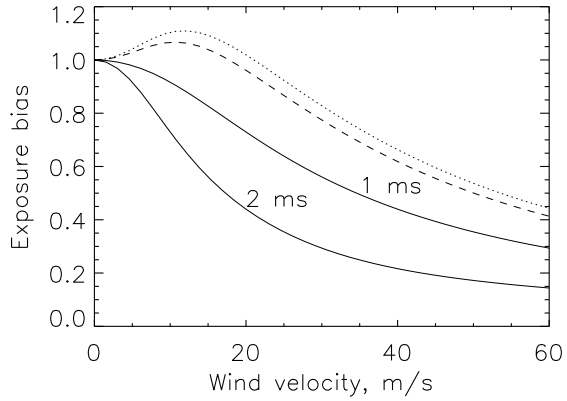

Fig. 4. Exposure time bias $R(\tau, z)$ (Eq. 16) for normal and differential scintillation as a function of single layer wind velocity (full lines). The suggested bias corrections are plotted as dotted (correction 1) and dashed (correction 2) lines. Left: normal SI, $R(\tau)$ for a 10 cm aperture, a layer at $z = 15$ km, and exposure times of 5 and 10 ms. Right: $R(\tau, z)$ for DSI with 4 and 2 cm apertures, layer at $z = 5$ km, exposure times 1 and 2 ms. The bias depends only on the $V\tau$ product, hence the curves for different exposure times can be obtained from each other by horizontal stretching.

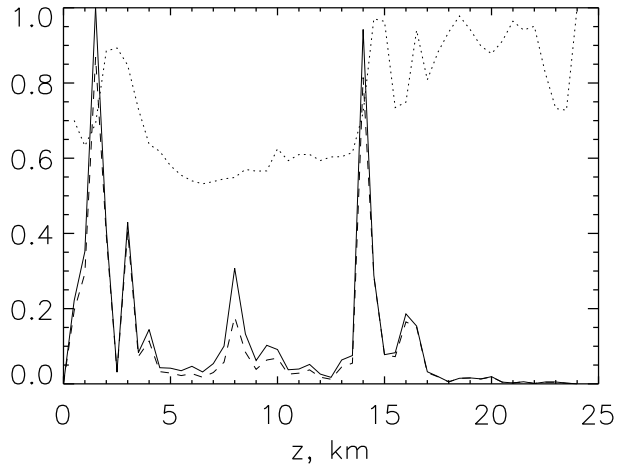

Fig. 5. For a true turbulence and wind profile with 0.5 km resolution, the relative contribution of layers to the DSI as measured with 4 and 2 cm apertures is plotted in solid line. This contribution is proportional to $C_n^2(z)Q(z)$. The dashed line shows the reduced contribution with a 1 ms exposure time. Exposure time bias $R(1ms)$ is plotted as dotted line.

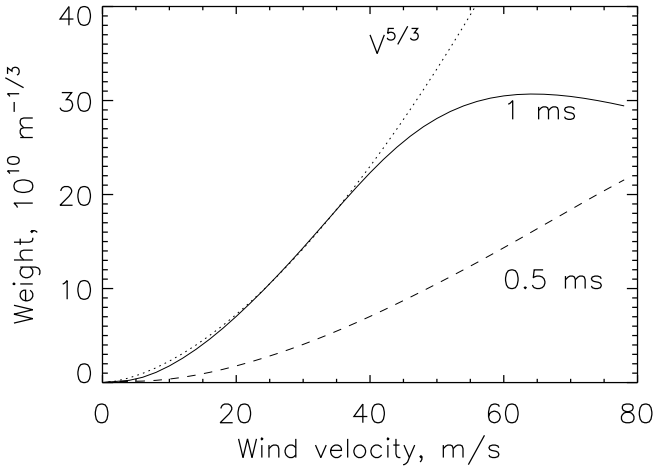

Fig. 6. Weighting functions for DESI are plotted against wind speed for exposure times 1 and 3 ms (full line), and 0.5 and 1.5 ms (dashed line). A single layer at 10 km and circular aperture of 1 cm diameter are assumed. Dotted line shows the $V^{5/3}$ law.

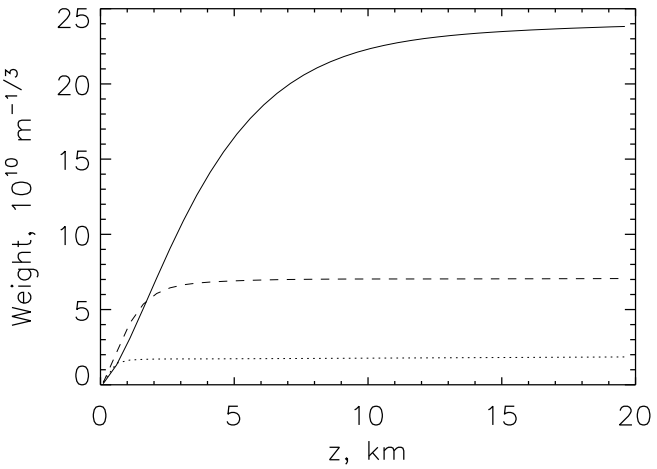

Fig. 7. Weighting functions for DESI. Exposure time 1 and 3 ms, aperture diameter 1 cm, wind speed 40 m/s (full line), 20 m/s (dashed line) and 10 m/s (dotted line).

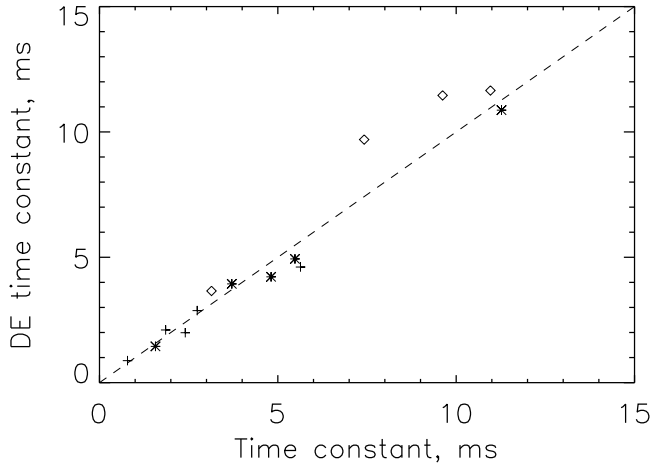

Fig. 8. Atmospheric time constant τ_a is compared to its estimate τ_{de} for the 5 real turbulence profiles measured by balloons at Cerro Pachon on nights with different conditions (asterisks). The same profiles were processed by increasing or decreasing the wind velocities by 2 times (pluses and diamonds, respectively).